$$= |\Gamma_d\Gamma_c - 1| \left|\frac{\partial}{\partial \omega}(\Gamma_d\Gamma_c)\right| \sin(\theta_a - \theta_b) \quad (7c)$$

where $\theta_a \equiv \angle(\Gamma_d\Gamma_c - 1)$ and $\theta_b = \angle \partial/\partial\omega_0(\Gamma_d\Gamma_c)$. Using (7), σ was calculated and compared to the exact values for circuits A and B in Fig. 1. Errors of 6% and 8% were obtained independent of the values used for C and L. The main point of interest in this section is the sign of σ. A positive σ means that a pole of (3) is in the right half plane and therefore the circuit is unstable.

A convenient graphical criterion for determining the sign of σ can be found by manipulating by the right hand side of (7) where, as noted previously, all quantities are evaluated at ω_0 as defined by (5a). Note that the condition $|\Gamma_d||\Gamma_c| > 1$ indicates instability only if the imaginary part of the frequency derivative in (7a) is positive. This last condition is violated in circuit B. The expression in (7c) indicates a graphical method of determining stability. Referring to Fig. 3, first form a vector which is tangent to the $\Gamma_d\Gamma_c$ curve at ω_0 and pointing in the direction of increasing ω. The angle $\theta_a - \theta_b$ is swept by turning this vector in a counterclockwise direction around its origin to the direction of the vector that points from 1 to $\Gamma_d\Gamma_c$ at ω_0. The angle is indicated in Fig. 3. Equation (7c) therefore shows that the only requirement for instability is that $180° > \theta_a - \theta_b > 0$. This would replace the not always valid equation (1).

A more convenient graphical approach can be determined for the typical case where a circuit can be split in such a way that Γ_d is approximately constant relative to the frequency dependence of Γ_c. By manipulating the expression in (7b), the following expression for instability can be written:

$$\mathrm{Im}\left[\left(\Gamma_c - \frac{1}{\Gamma_d}\right)\left(\frac{\partial}{\partial \omega}\Gamma_c\right)^*\right] > 0. \quad (8)$$

If $\phi_a \equiv \angle(\Gamma_c - 1/\Gamma_d)$ and $\phi_b \equiv \angle(\partial\Gamma_c/\partial\omega_0)$, criterion (8) can be simplified to

$$\sin(\phi_a - \phi_b) > 0. \quad (9)$$

Referring to Fig. 7, form a vector which points from the point $1/\Gamma_d$ to the point $\Gamma_c(j\omega_0)$. The direction of this vector defines ϕ_a. Draw another vector tangent to the Γ_c versus ω curve at ω_0 pointing in the direction of increasing ω_0. The direction of this vector defines ϕ_b. The angle $\phi_a - \phi_b$ is swept by turning the latter vector counterclockwise around the point $\Gamma_c(j\omega_0)$ until it is pointing in the direction of the former vector. If $180° > \phi_a - \phi_b > 0$, the circuit has a right half plane pole near ω_0 and is therefore unstable. This graphical method is usually more convenient than the one in the previous paragraph since it deals with quantities which remain inside the $|\Gamma| = 1$ circle. However, it does assume that Γ_d is approximately frequency independent.

IV. Conclusion

In this paper we have shown that a commonly used condition for instability is not universally valid. The Nyquist stability criterion has been written in a form that is convenient for microwave usage. A technique for producing Nyquist plots on commercially available microwave CAD packages has been described. An approximate expression was derived which locates a complex pole existing near a circuit resonance. Lastly, a graphical test was described for determining whether a circuit will start oscillating near a particular resonance frequency.

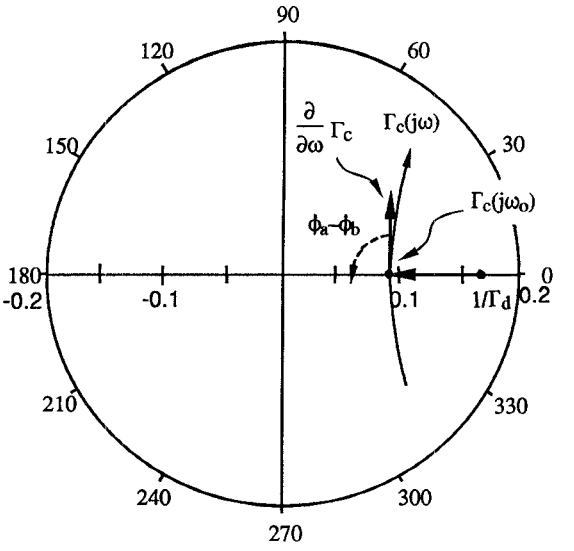

Fig. 7. Illustration of a graphical evaluation of stability near a resonance. The plot corresponds to the unstable circuit B in Fig. 1.

Acknowledgment

The author gratefully acknowledges several helpful discussions on this topic with Professor K. D. Stephan at the University of Massachusetts.

References

[1] B. P. Lathi, *Signals, Systems and Communication*. New York: Wiley, 1965, pp. 299–310.

[2] K. K. Kurokawa, "Some basic characteristics of broad band negative resistance oscillator circuits," *Bell Sys. Tech. J.*, vol. 48, no. 6, pp. 1937–1955, July 1969.

[3] D. J. Esdale and M. J. Howes, "A reflection coefficient approach to the design of one port negative impedance oscillators," *IEEE Microwave Theory Tech.*, vol. *MTT-29*, no. 8, pp. 770–776, Aug. 1981.

A General Approach for the *S*-Parameter Design of Oscillators with 1 and 2-Port Active Devices

R. D. Martinez and R. C. Compton

***Abstract*—This paper introduces a circular function that serves as a basis for deciding if a circuit will continuously oscillate. The circular function is derived from the signal flow graph of the circuit including the external load. Any node in the flow-graph can be split into two nodes, one of which contains incoming branches and the other containing outgoing branches. The circular function is then the transfer function between the two nodes, and it can be measured or simulated by looking at the reflection coefficient of a circulator inserted at the node that was originally split. Oscillations occur when the circular function is unity. Stability of these oscillations is determined by con-**

Manuscript received June 24, 1991; revised November 8, 1991. The work peformed at Cornell University was supported by GE, the U.S. Army Research Office and the DARPA Consortium for Superconducting Electronics (MDA972-90-C-0021).

The authors are with the School of Electrical Engineering, Cornell University, Phillips Hall, Ithaca, NY 14853.

IEEE Log Number 9105706.

sidering the behavior of the circular function as the circuit saturates. The circular function can be elegantly applied to 1-port oscillators that use negative resistance devices and to feedback oscillators containing transistors, and it reduces to previously published results for specific circuit topologies. To verify the practicality of this approach two 30 GHz HEMT oscillators were designed and tested.

Introduction

Analysis of feedback oscillators and negative resistance oscillators is traditionally performed using two different approaches. Frequently, Kurokawa [1] analysis is employed for 1-ports, and the Barkhausen [2] criterion is used for 2-ports. But the distinction between the two types is not rigorous. During operation, both share the concept of a sinusoidal wave being returned in phase with the same amplitude. The circular function, introduced in this paper, uses this concept to unify feedback and negative resistance oscillator analysis. This function provides an intuitive approach to the design of microwave oscillators. As a special case, the circular function encompasses results of stability for negative resistance devices [1], [3] and oscillation conditions [4], [5].

A circular function is the transfer function from a node's output to its input. The function describes the manner in which signals circulate through the circuit. Each time the signal circulates, the amplitude and phase of the node changes. The circular function has three main properties: existence, invariance, and stability. If the circular function is unity, a wave exiting from a circuit node returns to the node unchanged, and the circuit has the potential to oscillate. If such a condition *exists* at one node, other nodes in the circuit will also have unity circular functions. Under specific conditions the oscillation is *invariant*, regardless of the node being analyzed. The circuit will oscillate continuously if the potential oscillation is *stable*. Previous stability criteria assumed the frequency dependence of the active device vary slowly relative to the passive components [6]. But this assumption is no longer a concern since the circular function encompasses the frequency dependence of the active device. In the following text, each property will be rigorously explained and justified. Examples of 1-port and 2-port oscillator applications will be given. To determine stability, a simple large signal model for FET's is presented, and results from two 30 GHz HEMT feedback oscillators are presented at the end of this paper. Lumped circuit elements are not assumed, so this new analysis includes distributed systems.

Circular Function Definition

The definition of a circular function requires "splitting" a node. As in Fig. 1(a), an arbitrary node in a signal flow graph (SFG) may have signals entering, i_n, and exiting, k_n. A node is split by separating its inputs and outputs. The inputs are drawn entering a new node and the outputs exiting another new node as in Fig. 1(b). By connecting the input node to the output node with a branch of gain one, a unit branch, any transfer function in the SFG remains the same.

Fig. 1(c) illustrates the circular function τ of the node in Fig. 1(a). The circular function (c-function) is found by splitting the node as in Fig. 1(b), and removing the unit branch connecting the input and output node. The transfer function from the output node to the input node is the circular function. Note that each node has a corresponding circular function, so there are many circular functions in a SFG. Recall that the state of a node in a signal flow graph for scattering parameters represents the amplitude and phase of a sinusoidal wave.

Existence of an Operating Point: *If a node's c-function equals one and its state is nonzero, the circuit can oscillate.* A practical oscillator circuit contains an active device that has amplitude dependent S-parameters. As will be described later, the amplitude dependence determines continuous oscillation. A sinusoidal signal present at a node moves from the output node to the input node with the gain of the c-function. Next, the signal returns back to the output node from the input via the unit branch. This unit branch was the same branch removed earlier to find the c-function. Therefore a signal at the node continues to circulate unchanged if the c-function equals one; and the circuit oscillates.

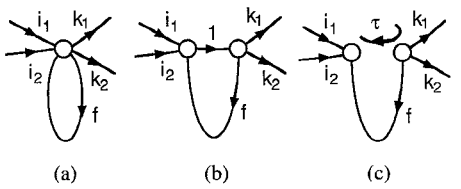

Fig. 1. (a) Arbitrary node in signal flow graph has inputs, i_n, and outputs, k_n. (b) To split, create an input node on left, and output node, on right; then connect them with a unit branch. (c) Remove the unit branch to find the circular function for the node.

Another justification for existence lies in the preliminaries of frequency domain Hopf bifurcation [7], [8]. If an open loop transfer function, the c-function in this case, is unity at the frequency ω_0, the associated time domain system has two imaginary eigenvalues of $\pm j\omega_0$. Thus the time domain system has a solution of the form $\sin \omega_0 t$, and the solution oscillates.

Invariance: *If a node's c-function equals one, then any other-node has a c-function of one, provided the nodes have nonzero transfer functions.* The proof is as follows. Suppose two arbitrarily chosen nodes, X and Y in Fig. 2(a), are split as in Fig. 2(b). Regarding the rest of SFG in the figure, four parameters, a, b, c, and d, completely represent the circuit. Using Mason's rule [9] and assigning τ as the c-function for node X and γ for node Y, the c-functions become

$$\tau = c + \frac{ab}{1-d} \qquad \gamma = d + \frac{ab}{1-c}. \tag{1}$$

Suppose node X has a known c-function of one, $\tau = 1$, then ab becomes

$$\tau = 1 = c + \frac{ab}{1-d} \rightarrow (1-c)(1-d) = ab \tag{2}$$

Substituting this value of ab into the definition of γ in (1):

$$\gamma = d + \frac{ab}{1-c} = d + \frac{(1-c)(1-d)}{(1-c)} = 1 \tag{3}$$

Assuming a and b are nonzero the c-function for Y is one, $\gamma = 1$ if $\tau = 1$. Note the inverse is also true, $\tau = 1$ if $\gamma = 1$. If a or b were zero and $\tau = 1$, nothing could be said of γ, other than $\gamma \neq 1$ is possible. If X and Y were nonzero states and a and b were nonzero transfer functions, $c = 1$ or $d = 1$ would lead to contradictions in Fig. 2(b). The existence and nonzero transfer functions preclude the $c = 1$ or $d = 1$ case for invariance.

Applying invariance of the c-function yields the same oscillation conditions [4], [5]. For example, suppose S-parameters s_{11}, s_{21}, s_{12}, and s_{22} represent a common gate FET with inductive feedback in the gate, and it is terminated with Γ_{in} on port 1 and Γ_{out} on port 2. To simplify the discussion, define the modified s_{11} and s_{22}:

$$s'_{11} = s_{11} + \frac{s_{21}\Gamma_{out}s_{12}}{1 - s_{22}\Gamma_{out}} \qquad s'_{22} = s_{22} + \frac{s_{12}\Gamma_{in}s_{21}}{1 - s_{11}\Gamma_{in}} \tag{4}$$

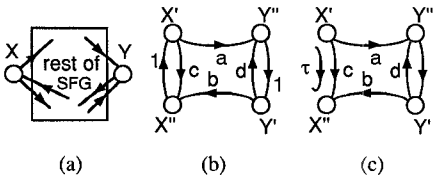

Fig. 2. (a) Two arbitrary nodes in a signal flow graph, SFG. (b) The nodes are split and four parameters characterize the rest of the SFG. (c) Analysis of the c-function τ, for the node X.

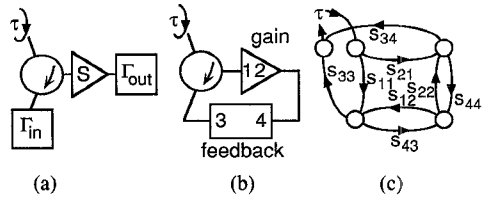

Fig. 3. (a) Arrangement to obtain the c-function, τ, for a negative resistance oscillator using a circulator. Active device S and load Γ_{out} form a negative resistance, and Γ_{in} is a passive load. (b) Arrangement to obtain the c-function of a feedback oscillator. Ports 3 and 4 are the feedback section, and ports 1 and 2 are the gain section. (c) Signal flow graph for the feedback oscillator of Fig. 3(b).

Now the c-function for the incident wave on port 1 becomes $s'_{11}\Gamma_{in}$ and for port 2 becomes $s'_{22}\Gamma_{out}$. From the properties of a c-function, if $s'_{11}\Gamma_{in} = 1$ then $s'_{22}\Gamma_{out} = 1$ provided s_{21} and s_{12} are nonzero. By existence, the circuit can oscillate if either c-function equals one. Consider the two port transistor terminated with a one port load as a negative resistance oscillator. Fig. 3(a) is a configuration for measuring the c-function of this negative resistance oscillator. By terminating the transistor S with the load Γ_{out}, the modified input reflection coefficient, s'_{11}, is on one port of the circulator and on the second port is Γ_{in}. Now the reflection coefficient τ at the third port is identical to the c-function for the wave incident on the transistor input, $s'_{11}\Gamma_{in}$. For an oscillator, one designs the loads and inductive feedback to obtain a c-function of one, $\tau = 1$, at the desired frequency and amplitude.

Obtaining a c-function for a feedback oscillator is not as obvious. Breaking the connection between the gain section and the feedback section gives access to a c-function. Attaching either end to the circulator (see Fig. 3(b)) makes the reflection coefficient τ identical to the c-function for the node representing the wave incident on the gain section. Fig. 3(c) is a signal flow graph of the feedback oscillator and circulator, which clearly shows the c-function being analyzed. The same properties of the c-function apply to the feedback oscillator: one designs the feedback and gain such that the c-function is one, $\tau = 1$, at the chosen frequency and amplitude. But different from the negative resistance oscillator, the wave incident on the gain input should not be reflected to the circulator. Instead, the wave should be amplified by the gain, pass through the feedback, and then returned to the circulator.

The existence and invariance property of the c-function form an oscillator test—provided one judiciously applies the nonzero exception of each property. To find the c-function, one simply breaks a connection and attaches the two ends to a circulator. The c-function is the reflection coefficient of the remaining third port.

Stable Oscillation for the Circular Function

Designing an oscillator requires knowledge of the signal's frequency and amplitude, which have been ignored to simplify the discussion. The c-function will vary in any physical circuit, so characterizing the stability of the operating point becomes as important as the existence of an operating point. For a sinusoidal signal of amplitude A, frequency ω, and phase ϕ, Kurokawa [1] has showed replacing ω with (5) leads to the stability criterion:

$$\omega + \frac{d\phi}{dt} - j\frac{1}{A}\frac{dA}{dt}. \tag{5}$$

The c-function has been written implicitly dependent on amplitude and frequency, but further references to the c-function will show explicit dependence. A c-function, $\tau(A, \omega)$, can oscillate at the operating point (A_0, ω_0) if

$$\tau(A_0, \omega_0) = 1 \tag{6}$$

Suppose the c-function, $\tau(A(t), \omega)$, oscillates in the neighborhood of ω_0, but the amplitude suffers a small perturbation at $t = 0$:

$$A(t) = A_0 + \delta A(t) \quad \text{where} \quad \delta A(t) \neq 0 \quad \text{at} \quad t = 0 \tag{7}$$

If the operating point is stable, the perturbing function $\delta A(t)$ will decay to zero for $t > 0$. Kurokawa has used the ω replacement to derive the stability criterion for two parallel impedances. In a similar manner, the operating point is stable if

$$\lim_{t\to\infty}\left(A_0 + \delta A(t),\ \omega_0 + \frac{d\phi}{dt} - j\frac{1}{A_0}\frac{d\delta A}{dt}\right) = 1. \tag{8}$$

Assuming $d\phi/dt$ and $A_0^{-1}\, d\delta A/dt$ are small compared to ω_0, a two parameter Taylor's expansion of $\tau(A, \omega)$ yields

$$\frac{\partial\tau}{\partial A}\delta A + \frac{\partial\tau}{\partial\omega}\left[\frac{d\phi}{dt} - \frac{j}{A_0}\frac{d\delta A}{dt}\right] = 0 \tag{9}$$

where the partial derivatives are evaluated at (A_0, ω_0). Using the imaginary part of (9) to solve for $d\phi/dt$ and substituting this into the real part of the equation yields an expression of δA and $d\delta A/dt$ (given in the Appendix):

$$A_0\left|\frac{\partial\tau}{\partial\omega}\right|^{-2}\operatorname{Im}\left\{\left(\frac{\partial\tau}{\partial\omega}\right)\left(\frac{\partial\tau}{\partial A}\right)^*\right\}\delta A + \frac{d\delta A}{dt} = 0. \tag{10}$$

Equation (10) is a first order differential equation for δA in time, and its solution is:

$$\delta A(t) = \exp\left[-tA_0\left|\frac{\partial\tau}{\partial\omega}\right|^{-2}\operatorname{Im}\left\{\left(\frac{\partial\tau}{\partial\omega}\right)\left(\frac{\partial\tau}{\partial A}\right)^*\right\}\right]. \tag{11}$$

Assuming $|\partial\tau/\partial\omega|$ is nonzero and A_0 is positive, the perturbing function, $\delta A(t)$, will exponentially decay to zero if:

$$\operatorname{Im}\left\{\left(\frac{\partial\tau}{\partial\omega}\right)\left(\frac{\partial\tau}{\partial A}\right)^*\right\} > 0. \tag{12}$$

Or more simply, the angles in the complex plane determine stability:

$$0° < \operatorname{Arg}\left\{\frac{\partial\tau}{\partial\omega}\right\} - \operatorname{Arg}\left\{\frac{\partial\tau}{\partial A}\right\} < 180°. \tag{13}$$

Stability: *If the angle from $\partial\tau/\partial A$ to $\partial\tau/\partial\omega$, measured in a counterclockwise directions, is less than 180°, the operating point is stable.* This stability criterion agrees with the specific case for a negative resistance oscillator [3]. Ideally, these partial derivatives should be evaluated at the operating point, but near the operation point is usually adequate.

The derivatives of the c-function are a measure of an oscillator's stability. Numerical simulations indicate that a large magnitude for the frequency derivative, $\partial\tau/\partial\omega$, correlates with a low phase noise. However, additional work is required to determine if the c-function can be used as a quantitative measure of the oscillator phase noise.

Special Case: Negative Resistance Oscillators with Constant Loads

To illustrate (13), suppose a negative resistance device with reflection coefficient $\rho(A, \omega)$ and a constant load with reflection coeffcient Γ form the c-function, $\tau(A, \omega) = \rho(A, \omega)\Gamma$. Since the load is constant, the existence and stability condition become, respectively:

$$\rho(A_0, \omega_0) = \frac{1}{\Gamma} \operatorname{Im}\left\{\left(\frac{\partial \rho}{\partial \omega}\right)\left(\frac{\partial \rho}{\partial A}\right)^*\right\} > 0. \tag{14}$$

Note the stability condition on the reflection coefficient $\rho(A, \omega)$ with a constant load is the same as the c-function, $\tau(A, \omega)$. In the case where the constant load matches the normalized impedance of the Smith chart, $\Gamma = 0$, the existence condition requires an undefined value for $\rho(A_0, \omega_0)$. The operating point is found by changing the normalizing impedance of the Smith chart so Γ is nonzero and $\rho(A_0, \omega_0) = 1/\Gamma$ is defined. But for circuits that oscillate with $\Gamma = 0$ loads, one observes that as the frequency increases $\rho(A, \omega)$ moves counterclockwise in the neighborhood of (A, ω_0). In addition, $|\rho(A, \omega_0)|$ increases towards infinity to satisfy the existence condition as the signal amplitude increases. This agrees with the stability criterion. Since $\partial\rho/\partial A$ points outwards from the origin of the Smith chart and $\partial\rho/\partial\omega$ is counterclockwise, the angle indicates stable oscillation (see Fig. 4). Suppose the conductance, G_D, of a voltage controlled negative differential device decreases as the signal level increases, $\partial G_D/\partial A < 0$ and $-G_D < 0$ [10]. If the conductance was initially large enough, $G_D > G_L$ where G_L is the load conductance, the conductance would decrease to satisfy $G_D = G_L$, and the load and device would oscillate in a parallel resonance circuit. Had the conductance been too small, $G_D < G_L$, the device could not satisfy the existence condition at any signal level. In these two cases, $G_D > G_L$ and $G_D < G_L$, stability was satisfied so existence ($G_D = G_L$) determines if the circuit will oscillate. Now consider a circuit with an inductor of $-j0.2G_L$ and capacitor of $+j0.2G_L$ in series with a parallel combination of G_D, $+jG_L$, and $-jG_L$. (All imaginary conductances are specified at the same frequency.) When the initial conductance is small, $G_D < G_L$, neither existence or stability are satisfied. But when the initial conductance is large enough to satisfy existence, $G_D > G_L$, the circuit fails the stability criterion (see Table I). By duality, four similar cases appear with series resonance. Distinguishing between current or voltage controlled negative resistance is extremely important since it dictates whether the conductance or resistance magnitude decreases to zero when the device saturates [11].

Simulating for Amplitude Dependence

For stability evaluation, both frequency dependence are needed. Ideally, large signal models or S-parameter measurements should be available, but most data sheets and models only provide small signal frequency dependence. If variable attenuators were placed before or after the small signal model of a transistor, the amplification could be reduced by increasing the attenuation. But such a scheme would not represent an increasing signal level because the attenuator changes every parameter: s_{11}, s_{12}, s_{22}, and s_{21}. If large signal models and data are unavailable, Pucel [12] and Johnson [13] have shown that changing the *magnitude* of a FET's forward transmission, $|s_{21}|$, accurately represents a changing signal level in a common source configuration. Simulating this on a linear simulation package is easy with a variable attenuator, a special 3-port, and a matched isolator that has 90° phase delay. By replacing a FET with the arrangement of Fig. 5(a), one can evaluate stability.

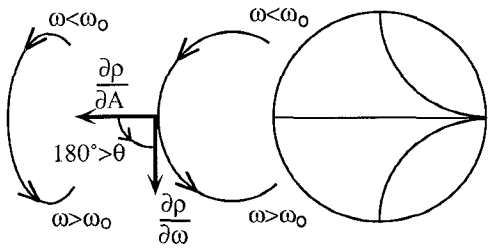

Fig. 4. Diagram showing the reflection coefficient as a function of frequency. As the oscillator saturates the counter-clockwise loop expands to infinity.

TABLE I
Four Example Cases of Existence and Stability

Circuit Description	Init. Conductance	Tests: √ ≡ pass, × ≡ fail: Existence	Stability	Refl. Coef. †
G_D, $+jG_L$, $-jG_L$ in parallel	$G_D > G_L$	√	√	CCW
	$G_D < G_L$	×	√	CW
$+j0.2G_L$ & $-0.2jG_L$ in series with circuit above	$G_D < G_L$	×	×	CCW
	$G_D > G_L$	√	×	CW

† Direction, clockwise (CW) or counter-clockwise (CCW), of reflection coefficient trajectory as frequency increases. The reflection coefficient plane is normalized to G_L

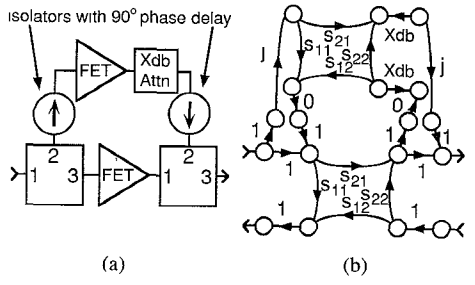

Fig. 5. (a) Configuration for simulating large signal characteristics of a FET. Reducing the attenuation simulates a larger signal. (b) An equivalent signal flow graph, the special 3-ports have s_{31}, s_{13}, s_{21}, and s_{32} equal to one.

With large attenuation, $X \approx 40$ dB, the FET in the top of Fig. 5(a) becomes completely isolated and the circuit is a small signal model. With less attenuation a signal moves through the upper path and then adds destructively (180° out of phase) to output of the lower FET; the circuit simulates saturation. Decreasing the attenuation reduces the forward transmission, and it indicates the direction of $\partial\tau/\partial A$. Starting with a large attenuation, one reduces the attenuation so the c-function is one, $\tau = 1$. If the attenuation is slightly reduced again, the point before reduction to the point after is the direction of $\partial\tau/\partial A$. This model can not represent extremely large amplitudes, such as the gate input being forward biased. But to design oscillators, this model can determine stability and approximate the amplitude at the operating point.

Feedback Oscillators

Negative resistance oscillators circulate a reflected wave using two 1-ports, whereas feedback oscillators circulate a transmitted

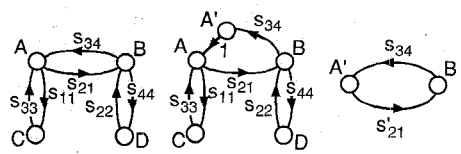

Fig. 6. (a) Signal flow graph (SFG) of feedback oscillator, neglecting reverse transmission. (b) Equivalent SFG by duplicating node A. State A is equivalent to A'. (c) Equivalent SFG by incorporating terms into s'_{21}.

wave through two 2-ports. Each 2-port has its output connected to the other's input. The c-function for the feedback oscillator of Fig. 3(c) is easy to simulate but the analytical form is complicated. Using the port numers of Fig. 3(c), Fig. 6(a) shows the signal flow graph of a feedback oscillator with the reverse transmissions of the gain and feedback sections neglected. Without affecting any result, the node representing the waves incident on the gain section, node A, is duplicated as in Fig. 6(b). The c-function for node A' becomes:

$$\tau(A, \omega) = s'_{21} s_{34}$$

where

$$s'_{21} = \frac{s_{21}}{1 - s_{11} s_{33} - s_{22} s_{44} + s_{11} s_{33} s_{22} s_{44}} \tag{15}$$

Now the c-function for the feedback oscillator is the same as for a 1-port oscillator (see Fig. 6(c)). The feedback section is actually a lossless 3-port terminated with a load to make a lossy 2-port, so the feedback couples power away from the circuit. At high frequencies, the gain will limit the ability to meet the existence condition $s'_{21} s_{34} = 1$. Reducing the power coupled away will help, but the gain has an upper frequency limit. Conjugate matching the transistor, $s_{33} = s_{11}^*$ and $s_{44} = s_{22}^*$, will maximize s'_{21}, and aside from a factor s'_{21} will be the same as G_{pmax} of a transistor. Although this analysis has neglected reverse transmission, simulating as in Fig. 3(b) does not.

Two *Ka*-band feedback oscillator circuits were designed, built, and tested using this analysis technique. HEMTs with grounded source leads were wire-bonded to microstrip transmission lines patterned on 10 mil alumina substrates. The AlGaAs/GaAs HEMT's were fabricated by GE and had gate widths of 50 μm and gate lengths of 0.25 μm. E-field probes patterned on the substrate launch the output signal into rectangular waveguide underneath the substrate, and above the substrate is a sliding short to tune the probe. A linear transistor model extracted from 0.5–20 GHz S-parameter measurements was used to design the circuit at 35 GHz. At this frequency, simulations indicated the HEMT's would provide 7.5 dB of gain when matched to the feedback network. One of the oscillators built used a coupler (see Fig. 7(a)) to provide -5.5 dB of feedback, and the other used a bandpass filter and microstrip "Tee" (see Fig. 7(b)) to provide -3 dB of feedback. For these circuits, the 7.5 dB gain corresponds to s'_{21} of (15), and the feedbacks of -5.5 dB and -3 dB correspond to s_{34} of the coupler and bandpass circuits, respectively. Both circuits have a c-function greater than one, $|s'_{21} s_{34}| > 1$, and as the signal amplitude increases $|s'_{21} s_{34}|$ approaches unity to establish an operating point.

The operating point is a function of the feedback and the large signal characteristics of the the HEMT. By adjusting the feedback and using a large signal model, the amplitudes of the operating points could be evaluated to determine the best feedback for maximum power. With only the small signal model available, the feedback was designed to amplify the initial signal, $|s'_{21} s_{34}| > 1$. In addition, the lengths of the excess transmission lines attaching the feedback and gain were adjusted to retain the phase of the signal $\angle s'_{21} s_{43} = 0°$, which is an implicit requirement of (6). The bandpass oscillator operated at 28.3 GHz with 0.1 mW of output power, and the coupler oscillator operated at 31.4 GHz with 1.5 mW of power. During the simulation, the E-field probe was assumed to be a perfect 50 Ω load and the bias circuit to be a perfect RF open. In practice these components are not ideal, which is believed to be the major contributing factor for the reduced operating frequency.

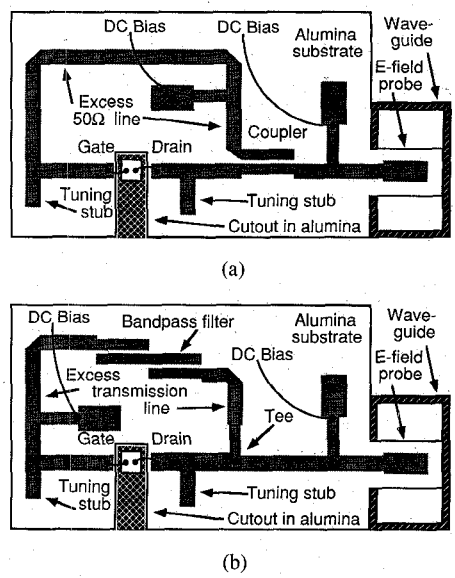

Fig. 7. Scale drawings of two HEMT oscillators. Using epoxy, HEMTs are glued to carrier exposed by cutouts in the alumina substrate. (a) The coupler provides feedback for the circuit to oscillate. (b) A bandpass filter selects the frequency to feedback.

Conclusion

The three properties of the c-function form a complete design test for oscillators. Existence and stability of the c-function's operating point determine oscillation. Both properties must be satisfied for the circuit to oscillate. Circular functions are easily available for simulation by inserting a circulator into any signal path. And the invariance property guarantees that any c-function can be used to determine existence and stability. The properties apply to all circuits so the difference between feedback and negative resistance oscillators is no longer important to evaluate oscillation.

Appendix

Assigning:

$$\frac{\partial \tau}{\partial \omega} = \tau_\omega^r + j\tau_\omega^i \quad \text{and} \quad \frac{\partial \tau}{\partial A} = \tau_A^r + j\tau_A^i. \tag{A1}$$

Then from (9):

$$(\tau_A^r + j\tau_A^i)\,\delta A + (\tau_\omega^r + j\tau_\omega^i)\left[\frac{d\phi}{dt} - \frac{j}{A_0}\frac{d\delta A}{dt}\right] = 0. \tag{A2}$$

By the imaginary part of (A2):

$$\tau_A^i\,\delta A - \frac{\tau_\omega^r}{A_0}\frac{d\delta A}{dt} + \tau_\omega^i \frac{d\phi}{dt} = 0 \rightarrow \frac{d\phi}{dt} = \left[\frac{\tau_\omega^r}{A_0}\frac{d\delta A}{dt} - \tau_A^i\,\delta A\right] \Big/ \tau_\omega^i. \tag{A3}$$

The real part of (A2) gives

$$\tau_A^r \delta A + \tau_\omega^r \frac{d\phi}{dt} + \frac{\tau_\omega^i}{A_0}\frac{d\delta A}{dt} = 0. \quad \text{(A4)}$$

By using (A3) form of $d\phi/dt$ into (A4):

$$\tau_A^r \delta A + \frac{\tau_\omega^r}{\tau_\omega^i}\left[\frac{\tau_\omega^r}{A_0}\frac{d\delta A}{dt} - \tau_A^i \delta A\right] + \frac{\tau_\omega^i}{A_0}\frac{d\delta A}{dt} = 0 \quad \text{(A5)}$$

$$\left(\tau_A^i - \frac{\tau_\omega^r}{\tau_\omega^i}\tau_A^i\right)\delta A + \left(\frac{\tau_\omega^i}{A_0} + \frac{(\tau_\omega^r)^2}{\tau_\omega^i A_0}\right)\frac{d\delta A}{dt} = 0 \quad \text{(A6)}$$

$$\frac{1}{\tau_\omega^i}[\tau_A^r\tau_\omega^i - \tau_\omega^r\tau_A^i]\,\delta A + \frac{1}{\tau_\omega^i A_0}[(\tau_\omega^i)^2 + (\tau_\omega^r)^2]\frac{d\delta A}{dt} = 0 \quad \text{(A7)}$$

if τ_ω^i is nonzero, multiply both sides by τ_ω^i, and use the imaginary operator:

$$\mathrm{Im}\left\{\left(\frac{\partial\tau}{\partial\omega}\right)\left(\frac{\partial\tau}{\partial A}\right)^*\right\}\delta A + \frac{1}{A_0}\left|\frac{\partial\tau}{\partial\omega}\right|^2\frac{d\delta A}{dt} = 0 \quad \text{(A8)}$$

$$A_0\left|\frac{\partial\tau}{\partial\omega}\right|^{-2}\mathrm{Im}\left\{\left(\frac{\partial\tau}{\partial\omega}\right)\left(\frac{\partial\tau}{\partial A}\right)^*\right\}\delta A + \frac{d\delta A}{dt} = 0 \quad \text{(A9)}$$

Acknowledgment

The authors thank P. M. Smith of GE for his advice and encouragement.

References

[1] M. J. Howes and D. V. Morgan, *Microwave Devices*. New York: Wiley, 1976, pp. 209–217.
[2] J. Millman, *Microelectronics*. New York: McGraw-Hill, 1979, pp. 647–648.
[3] D. J. Esdale and M. J. Howes, "A reflection coefficient approach to the design of one-port negative impedance oscillators," *IEEE Trans. Microwave Theory Tech.*, vol. MTT-29, no. 8, pp. 770–776, Aug. 1981.
[4] G. R. Basawapatna and R. B. Stancliff, "A unified approach to the design of wide-band microwave solid-state oscillators," *IEEE Trans. Microwave Theory Tech.*, vol. MTT-27, no. 5, pp. 379–385, May 1979.
[5] G. D. Vendelin, *Design of Amplifiers and Oscillators by the S-Parameter Method*. New York: Wiley, 1982, pp. 132–172.
[6] K. Kurokawa, "Injection locking of microwave solid-state oscillators," *Proc. IEEE*, vol. 61, no. 10, pp. 1386–1410, Oct. 1973.
[7] A. I. Mees and L. O. Chua, "The Hopf bifurcation theorem and its applications to nonlinear oscillations in circuits and systems," *IEEE Trans. Circuits Syst.*, vol. CAS-26, no. 4, pp. 235–254, Apr. 1979.
[8] D. J. Allwright, "Harmonic balance and the Hopf bifurcation," *Mathematical Proceedings of the Cambridge Philosophical Society*, vol. 82, pp. 453–467, 1977.
[9] S. J. Mason, "Feedback theory-further properties of signal flow graphs," *Proc. IRE*, vol. 44, pp. 920–926, July 1956.
[10] G. Gonzalez, *Microwave Transistor Amplifiers*. Englewood Cliffs, NJ: Prentice-Hall, 1984, pp. 194–199.
[11] S. M. Sze, *Physics of Semiconductor Devices*, 2nd ed. New York: Wiley, 1981, pp. 637–642.
[12] R. A. Pucel, R. Bera, and D. Masse, "Experiments on integrated gallium-arsenide FET oscillators at X-band," *Electron. Lett.*, vol. 11, no. 10, pp. 219–220, May 15, 1975.
[13] K. M. Johnson, "Large signal GaAs MESFET oscillator design," *IEEE Trans. Microwave Theory Tech.*, vol. MTT-27, no. 3, pp. 217–226, Mar. 1979.

Parameter Extraction Technique for HBT Equivalent Circuit Using Cutoff Mode Measurement

Seonghearn Lee and Anand Gopinath

Abstract—**We propose a new parameter extraction method based on the *S*-parameter measurements of the HBTs biased to cutoff. This method is applied to confirm the results for the RF probe pad and interconnection pattern parasitics obtained from the special test structures, and to determine some of the device capacitances of the HBT. The remaining device parameters are extracted by the *S*-parameter measurements of the devices biased to the active mode. The extraction technique gives good agreement between the equivalent circuit and the measured *S*-parameters of the HBT including probe pads and interconnections.**

I. Introduction

Heterojunction bipolar transistors (HBT's) are used in monolithic microwave integrated circuit (MMIC) applications. Accurate parameter extraction of their equivalent circuit is crucial for the development of HBT circuits and applications. These device equivalent circuits are derived from scattering (*S*)-parameter measurements [1]–[7] usually measured on discrete devices using "on wafer" RF probes over a range of frequencies and biases. For the "on wafer" probing, the additional RF probe pads and interconnections (RF probe-pattern) have to be added to the device, and their parasitics are included in the measurement. Computer optimization is used to fit the equivalent circuit parameters together with parasitics, to the measured *S*-parameters [5]–[7]. In general, it is necessary to reduce the number of unknown parameters to avoid the non-physical local minima which occur in this technique [7]. Thus, experimental determination of the parasitic parameters is the best method to achieve this reduction of the parameter space dimension. Usually, the RF probe-pattern (pads and interconnections) parasitics are ignored, and as a result, the agreement between the circuit *S*-parameters and measurements is often not very good. It is therefore necessary that an equivalent circuit model including the RF probe-pattern be used in this parameter extraction process.

In general, most of the equivalent circuit modeling results have been optimized without independent measurements of probe-pattern parasitics. RF probe-pattern parasitics may be predetermined by means of properly designed test structures [1], [8]. In a previous paper [9], we have introduced an accurate parameter extraction scheme for RF probe-pattern parasitics using the simultaneous optimization of "open" and "short" test structures. We have also proposed a new RF probe-pattern equivalent circuit model, and have demonstrated that this model overcomes some of the shortcoming of previous models [1], [2].

Fig. 1 shows the layout of a typical RF probe-pattern used to measure HBT's built at the University of Minnesota. The RF probe-pattern parasitics are determined by measuring two test structures, as discussed previously [9]: one is an "open" circuit structure that consists of RF probe pads and interconnections on the appropriate passivation layer (silicon nitride in our case), and the other is a

Manuscript received May 13, 1991; revised September 3, 1991.
The authors are with the Department of Electrical Engineering, University of Minnesota, 200 Union Street, S.E., Minneapolis, MN 55455.
IEEE Log Number 9105453.